

*J U Wren*

NATIONAL AERONAUTICS AND SPACE ADMINISTRATION

*Technical Report 32-1243*

*A New Deformation Mechanism in  
Pyrolytic Carbon at High  
Temperatures*

G. M. Jenkins

17

FACILITY FORM 602	N68-165261	
	(ACCESSION NUMBER)	(THRU)
	19	1
	(PAGES)	(CODE)
<i>CI-92748</i>	<i>18</i>	
(NASA CR OR TMX OR AD NUMBER)	(CATEGORY)	

JET PROPULSION LABORATORY  
CALIFORNIA INSTITUTE OF TECHNOLOGY  
PASADENA, CALIFORNIA

February 15, 1968

NATIONAL AERONAUTICS AND SPACE ADMINISTRATION

*Technical Report 32-1243*

*A New Deformation Mechanism in  
Pyrolytic Carbon at High  
Temperatures*

*G. M. Jenkins*

Approved by:



H. E. Martens, Manager  
Materials Section

**JET PROPULSION LABORATORY  
CALIFORNIA INSTITUTE OF TECHNOLOGY  
PASADENA, CALIFORNIA**

February 15, 1968

**TECHNICAL REPORT 32-1243**

Copyright © 1968

Jet Propulsion Laboratory  
California Institute of Technology

Prepared Under Contract No. NAS 7-100  
National Aeronautics & Space Administration

## **Foreword**

The author, G. M. Jenkins, is a Lecturer in Materials Science at the University College of Swansea, Swansea, United Kingdom. The paper was written while he was affiliated with the Jet Propulsion Laboratory during the summer of 1967. The appendix material was provided by R. B. Matthews, Associate Scientist of the Materials Research Group of the Materials Section, who is now at the University of Denver, Denver, Colorado, Department of Metallurgy.

**Page intentionally left blank**

**Page intentionally left blank**

## Contents

I. Introduction . . . . .	1
II. Overall Description of the Deformation . . . . .	1
III. Microstructural Description of Deformation: Model . . . . .	4
IV. Structure and Movement of Unit c-Axis Dislocations . . . . .	5
V. High-Strain, High-Temperature Deformation . . . . .	6
VI. Discussion . . . . .	6
Appendix. Etching and Transmission Electron Microscopy of Pyrolytic Carbon . . . . .	8
References . . . . .	12

## Figures

1. Schematic representation of general features associated with tensile deformation . . . . .	1
2. Pyrolytic graphite polished and etched on plane lying in direction of tensile stress, perpendicular to plane of deposition: (a) Before deformation, (b) After 25% deformation (200 X) . . . . .	2
3. As-cleaved surface in plane of deposition: (a) below 10% deformation, (b) At 30% deformation (200 X) . . . . .	2
4. Cleaved, hot-worked pyrolytic graphite, by scanning electron microscopy . . . . .	3
5. Unpolished side view of 27%-deformed specimen, by scanning electron microscopy (3,500 X) . . . . .	3
6. Features produced by oxidizing newly cleaved 30%-deformed specimen in air at 800°C (1,000 X) . . . . .	3
7. Typical dislocation pattern in hot-worked graphite: Transmission electron microscopy (10,000 X) . . . . .	3
8. Examples of interaction of basal-plane and c-axis screw dislocations . . . . .	4
9. Attenuated configuration of a c-axis screw after basal plane dislocations have moved through . . . . .	4
10. Cleavage features below 10% deformation (300 X) . . . . .	5
11. Atomic arrangements at the cores of unit c-axis dislocations . . . . .	5

## Contents (contd)

### Figures (contd)

A-1. Cathodically etched, longitudinal section of pyrolytic carbon tensile specimen [Polarized light (100 X)] . . . . .	9
A-2. Kink band of Fig. 1 (1000 X) . . . . .	10
A-3. Transmission electron photomicrograph of deformed pyrolytic carbon (20,000 X) . . . . .	11
A-4. Transmission electron photomicrograph of deformed pyrolytic carbon (21,000 X) . . . . .	12

## Abstract

It is demonstrated that the creep deformation of pyrolytic graphite at high temperatures in response to a stress in an  $a$ -direction may be the result of the independent, two-dimensional plastic distortion of each individual plane of carbon atoms. On the model, the distortion within each plane is produced by the movement of unit  $c$ -axis dislocations, mainly by climb from a generalized Herring-Nabarro mechanism. This distortion has some bearing on creep in polycrystalline graphite at high temperature and under neutron irradiation.



# A New Deformation Mechanism in Pyrolytic Carbon at High Temperatures

## I. Introduction

Plastic deformation of pyrolytic graphites in response to a stress in the  $a$ -direction at high temperatures has been demonstrated previously (Refs. 1, 2, and 3), and characteristics of the deformation behavior have been reviewed by Fischbach and Kotlensky (Ref. 4). The actual mechanism, however, was left open to speculation. It is important because it shows unambiguously that a mode of deformation other than basal-plane shear is possible in graphite at high temperatures and, thus, has bearing on the general overall plastic deformation observed in polycrystalline graphites at high temperatures and, possibly, under neutron irradiation.

## II. Overall Description of the Deformation

It has been shown (Ref. 1) that, when pyrolytic graphite is pulled in the plane of deposition above about 2500°C, the first stage of the deformation is the pulling flat of the characteristic growth cones in the direction of the tensile stress to produce undulations lying in this direction (Fig. 1). This fact is brought out clearly on etching sections cut perpendicular to the plane of depo-

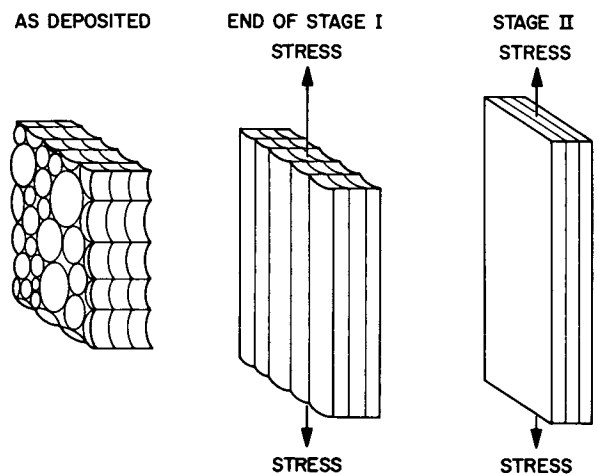
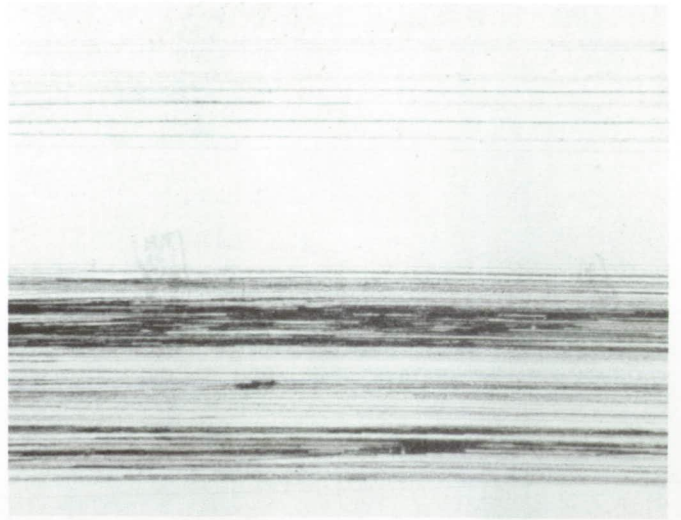
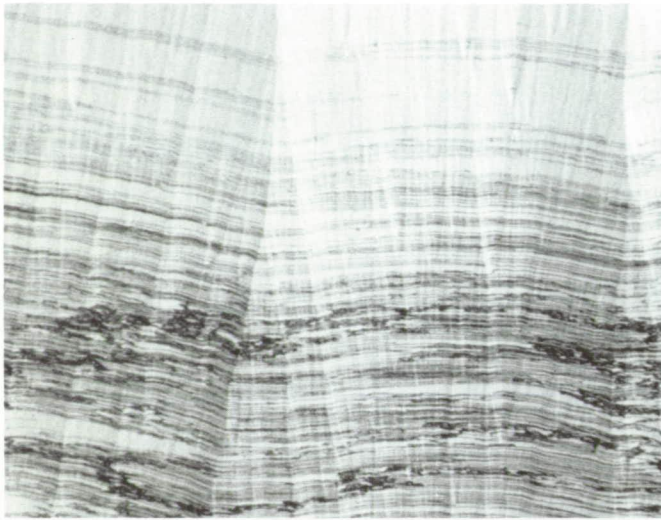
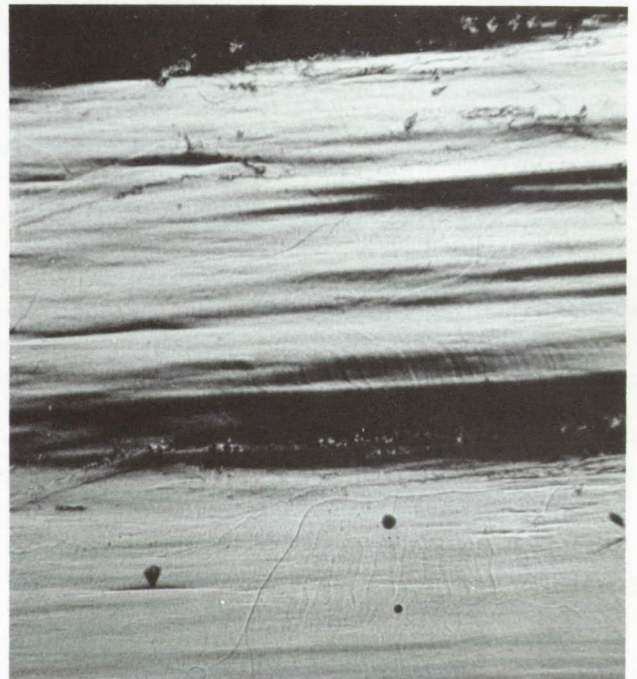
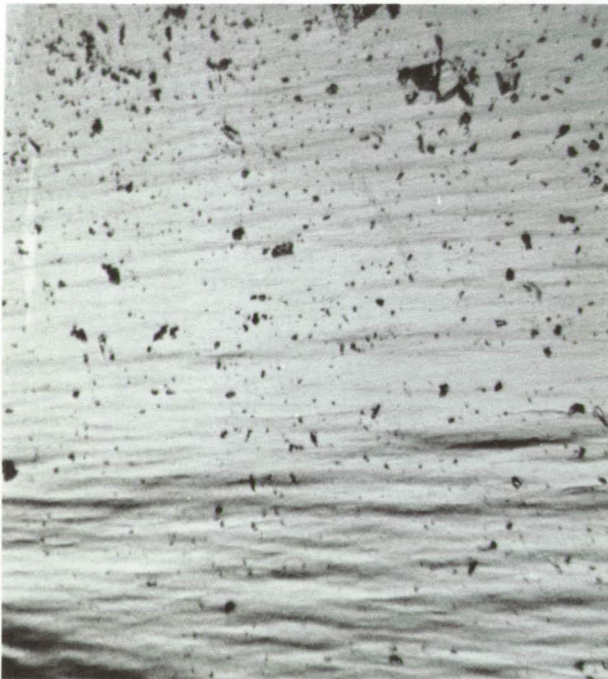


Fig. 1. Schematic representation of general features associated with tensile deformation

sition in the direction of the applied stress (Fig. 2). This process is observed up to the first 10% of deformation. Thereafter a smoother surface is observed – albeit with irregular undulations of different periodicity, again lying in the direction of the applied stress (Fig. 3). These features are brought out more clearly by electron scanning



**Fig. 2. Pyrolytic graphite polished and etched on plane lying in direction of tensile stress, perpendicular to the plane of deposition (a) Before deformation (b) After 25% deformation (200 X)**



**Fig. 3. As-cleaved surface in plane of deposition (a) below 10% deformation (b) At 30% deformation 200 X**



microscopy (Fig. 4). Electron scanning microscopy of an as-deformed tensile specimen gage-section surface perpendicular to the basal plane in the direction of the applied stress (Fig. 5) reveals that there are no general slip planes angled with respect to the basal plane. Etching of the basal plane of deformed samples, both by slow oxidation in air at 600°C and in sodium peroxide at 350°C, reveals a large number of randomly arranged, shallow,

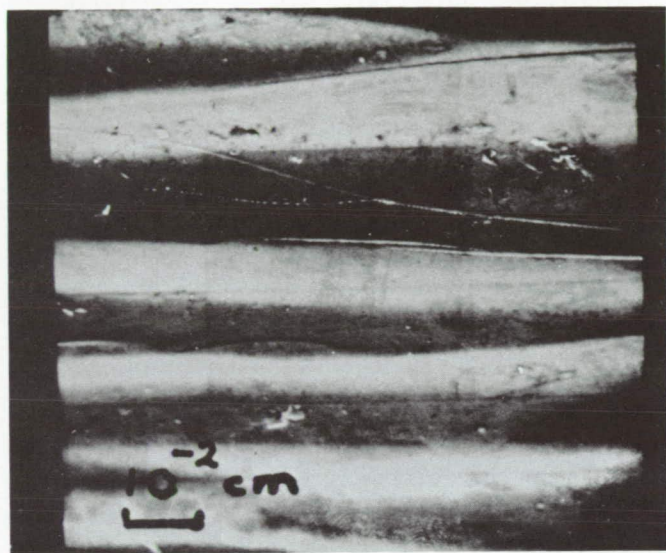


Fig. 4. Cleaved, hot-worked pyrolytic graphite, by scanning electron microscopy



Fig. 5. Unpolished side view of 27%-deformed specimen, by scanning electron microscopy (3,500 X)

etched pits (Fig. 6) with a population density of about  $10^8 \text{ cm}^{-2}$ . No sub-boundaries or slip systems are revealed. The pattern shown is close to that achieved by a similar technique, on presumably similar hot-worked pyrolytic graphite, by Sellar and Trillat (Ref. 5). Transmission electron microscopy of a material that is deformed 30% in elongation (Fig. 7) shows, again, that sub-boundaries

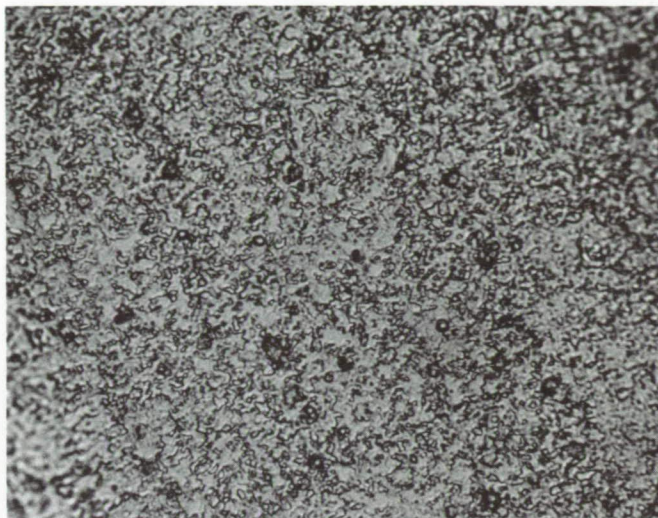


Fig. 6. Features produced by oxidizing a newly cleaved 30%-deformed specimen in air at 800°C (1,000 X)



Fig. 7. Typical dislocation pattern in hot-worked graphite: transmission electron microscopy (10,000 X)

on prism planes are not defined. Details of the experimental techniques are given in the Appendix.

To summarize, elongations of at least 30% are possible in the  $a$ -direction of pyrolytic graphite, and explanations for such distortions in terms of (1) pyramidal slip planes, (2) grain boundary sliding, and (3)  $c$ -axis line-defect movement do not seem to be adequate. An explanation that does seem to fit the facts is presented here.

### III. Microstructural Description of Deformation: Model

Pyrolytic graphite probably contains a large number of  $c$ -axis screw dislocations (*forest dislocations*), which are associated with the characteristic growth cones. As the temperature is raised and the basal planes are pulled in the  $a$ -direction, the planes will attempt to straighten themselves in the direction of the applied stress — which process must involve extensive shear in the basal plane. One may assume that the  $c$ -axis screws will be broken up only if the basal-plane dislocations are allowed to sweep through them.

Consider the basic interaction of a basal-plane and a  $c$ -axis screw dislocation (Fig. 8). To produce a shear strain in the  $x$ -direction, the basal-plane screw dislocation AB has to glide in the  $y$  direction and intersect the  $c$ -axis screw dislocation CD at E. A long-range elastic force of repulsion exists between the two dislocations. The dislocation AB has been shown to be glissile, while CD should be completely sessile. Slip can take place only if AB breaks completely through the forest dislocation

tion CD. This can be accomplished by the formation of a basal-plane kink at E and a  $c$ -axis kink in AB at the point of intersection. In order to glide past, the edge kink on AB must climb by either absorbing or emitting vacancies. The rate-determining process will, thus, be that of the migration of vacancies. Such migration requires a high-activation energy in graphite, estimated theoretically to be about 263 kcal/mole (Refs. 6 and 7), if one assumes the heat of sublimation of graphite is 170 kcal/mole. Kotlensky (Ref. 8) observed the activation energy of creep in the initial stages to be about 250 kcal/mole. As more dislocations pass through CD, the size and number of kinks will increase until the  $c$ -axis dislocation is drawn out in the direction of the tensile stress as shown in Fig. 9. The original dislocation CD is converted from a pure  $c$ -axis screw to a stepped-edge dislocation until the shear stresses in the growth cones — resolved from a tensile stress in the deposition plane — are negligible. The actual dislocation arrangement will, of course, be more complicated.

Cleavage of specimens with 10% elongation (Fig. 10) shows that, as expected from the dislocation arrangements, fracture proceeds stepwise, being held up at lines lying in the direction of the applied tensile stress. Such a fracture running perpendicular to the direction of stress travels along one particular plane of atoms that, say, act as the half plane to an edge dislocation with a  $c$ -axis Burgers vector, until the break reaches the end of the half-plane. The fracture will then prefer to travel along the core of the dislocation until the dislocation steps down in the  $c$ -direction, changing from edge to screw. Next, the crack is forced to travel on in its original direction until it comes to the edge of another half-plane, and so on. The loose flaps of graphite sheets produced by such an operation will tend to curl away, producing the effect seen in Fig. 10. At higher

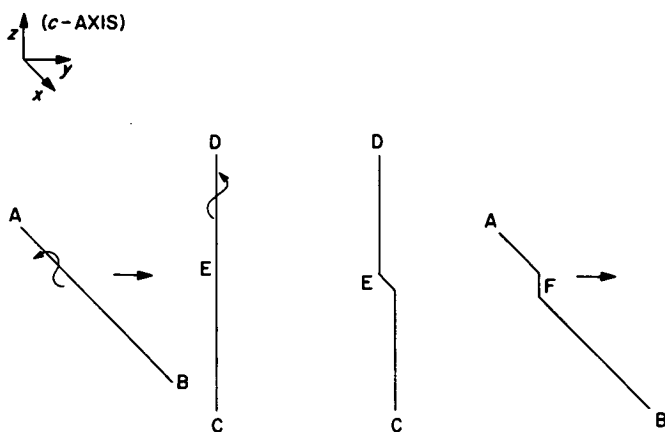


Fig. 8. Examples of interaction of basal-plane and  $c$ -axis screw dislocations

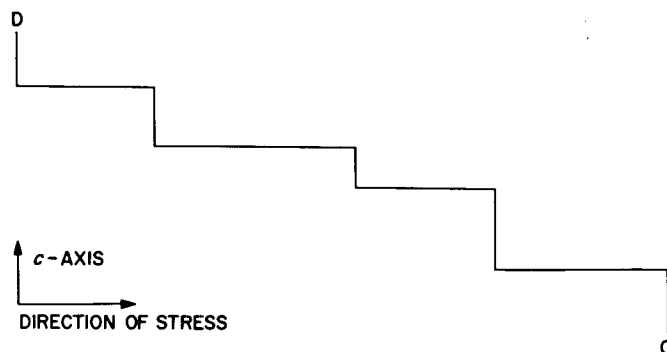


Fig. 9. Attenuated configuration of a  $c$ -axis screw after basal plane dislocations have moved through



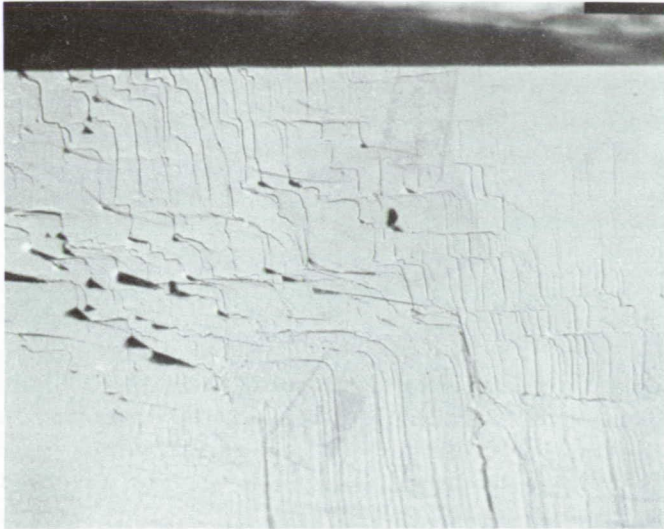


Fig. 10. Cleavage features below 10% deformation (300 ×)

deformations, the step fracture is not observed, but coiled-up sheets of graphite are present after cleavage, lying in the direction of the applied stress (Fig. 4). There is a probability that such cleavage will expose half planes of basal-plane dislocations with *c*-axis Burgers vectors. Thus, the unit *c*-axis dislocations resulting from the original line defects (AB in Fig. 8) will be distributed at random throughout individual layers. It will be profitable now to consider these unit *c*-axis dislocations in detail.

#### IV. Structure and Movement of Unit *c*-Axis Dislocations

Unit edge-dislocations with a line vector in the *c*-direction and a Burgers vector in one of three *a*-directions are restricted to a basal plane of carbon atoms and can be considered as point defects. The associated basal-plane dislocation can move very easily, even at low temperatures, and, therefore, can be neglected in any high-temperature energy consideration.

The core, which is completely sessile at room temperature, has very small dimensions and in this way is unlike basal-plane dislocations, which are very wide ( $\sim 50 \text{ \AA}$ ). There are two possible configurations as depicted in Fig. 11. Figure 11a shows an 8-sided defect, Fig. 11b a 10-sided defect. Configurations can change from one to the other, simply by absorbing or emitting vacancies. In doing so, they climb and contribute to a basal-plane distortion. It should also be noted that they could also glide in response to an applied shear on a prism plane, merely by the replacement of one bond by another which is

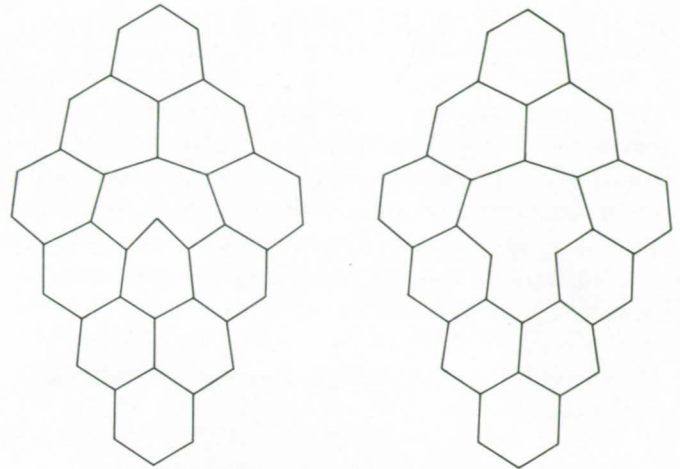


Fig. 11. Atomic arrangements at the cores of unit *c*-axis dislocations

equally strong. The activation energy in each case would be approximately equal to that required for vacancy movement. Judging by Fig. 6, the population of such defects, plus the remnants of *c*-axis screws, is of the order of  $10^8 \text{ cm}^{-2}$ .

In summary, unit dislocations may result from three conditions:

- (1) High-temperature breakup of *c*-axis edge dislocations by randomized vacancy climb
- (2) High-temperature interaction of basal-plane dislocations with *c*-axis screws
- (3) Collapse of lines of vacancies produced by neutron irradiation

Unit dislocations have the following functions:

- (1) Act as sources and sinks for vacancies and sinks for interstitials.
- (2) Pin dislocations with long-range strain fields.
- (3) Move by climb or glide to produce distortion of individual planes of carbon atoms.
- (4) Allow three-dimensional migration of interstitials.

Interstitials between one pair of layers will be attracted to the dangling bond. However, before climb can take place, bonds must be broken, so there will be a distinct probability of the interstitial's moving back between the original pair of planes or, with equal probability, of the interstitial's moving on in between the neighboring pair.

## V. High-Strain, High-Temperature Deformation

It has been shown that pulled, pyrolytic graphite contains a large number of point defects that can, if moved, produce distortions in individual planes of carbon atoms. At high temperatures ( $>2500^{\circ}\text{C}$ ) Fischbach and Kotlensky (Ref. 1) have shown that the basal-shear-flow stress of pyrolytic graphite drops from  $\sim 10^3$  to  $\sim 10^2$  lb/in.<sup>2</sup>, or less. At these high temperatures, the basal planes are much farther apart than at low temperatures because of the high *c*-axis expansion. The force of attraction of one layer to its neighbor at these temperatures must, therefore, be extremely small. Defect configurations in one plane will have very little relationship to neighboring ones, and each will deform independently. Under such conditions, the contribution of continuous *c*-axis dislocations to uniaxial distortion is extremely improbable. We are left to conclude that each plane distorts independently of its neighbors by the movement of unit *c*-axis dislocations, probably by differential climb governed by a generalized Herring-Nabarro mechanism. Friedel (Ref. 9) has worked out the mathematical relationships governing the strain rate  $\dot{\epsilon}$  caused by such creep in the presence of isolated dislocations.

$$\dot{\epsilon} = D\sigma b^3 / \{l^2 kT [\ln(l/b)]\}$$

where

$D$  = coefficient of self-diffusion via vacancies  
(in our case in one plane)

$l$  = average distance between dislocations

$b$  = Burgers vector

$\sigma$  = the applied stress

$k$  = Boltzmann constant

$T$  = absolute temperature

Under a stress of  $10^8$  dynes/cm<sup>2</sup>, source/sink population is  $10^8$  cm<sup>-2</sup>, assuming  $D \approx 10^{-12}$  s/cm<sup>-2</sup> at  $2350^{\circ}\text{C}$  (Ref. 7), and an activation energy for diffusion of 260 kcal at  $2350^{\circ}\text{C}$ ,  $\dot{\epsilon} \approx 3 \times 10^{-8}$  sec<sup>-1</sup>. At  $2550^{\circ}\text{C}$ , this will be  $\approx 3 \times 10^{-6}$  s<sup>-1</sup>, and at  $2750^{\circ}\text{C}$ ,  $\approx 3 \times 10^{-4}$  s<sup>-1</sup>.

These values are somewhat greater than those actually found by Kotlensky (Ref. 8) and Fischbach (Ref. 10). As climb proceeds, the population of *c*-axis dislocations will decrease as more and more move to the edge of the specimen or mutually annihilate. Thus,  $l$  should increase with time, and the creep rate should gradually decrease. Such a decrease has actually been observed. The stress

dependence has been estimated to be  $\approx 1.6$ , which is close to the unity predicted by the Herring-Nabarro mechanism. The fact that it is somewhat greater than unity may, perhaps, be ascribed to the contribution of glide mechanisms of individual unit *c*-axis dislocations.

It should be noted that in each layer of atoms we have plane-strain conditions. If fracture or cavity elongation occurs in one plane, the stress in that plane or in any other plane remains to a first approximation constant; therefore, the cavity growth is not catastrophic. Planes on either side of the growing hole in one plane will have time to collapse and mend such incipient fractures. In this way, the *c*-axis contraction, as well as the more easily understood *a*-axis contraction, can be accounted for. The undulations at high strains (Fig. 3b) may be manifestations of the instability inherent in pulling very thin sheets or piles of unbonded thin sheets.

## VI. Discussion

It has been demonstrated that the creep of hot-worked pyrolytic graphite may be ascribed to the movement of point defects, with each plane deforming independently of its neighbor. It has been contended previously by Jenkins and Williamson (Ref. 11) that the predominant mechanism of creep at high temperatures should be that of Herring and Nabarro, and the results on pyrolytic graphite in no way conflict with this opinion.

Green and Zukas (Ref. 12) have shown that the stress-dependence coefficient of polycrystalline graphite is between  $\sim 5.5$  and  $8.0$ . In this case, it is clear that the Herring-Nabarro mechanism is not the only mode of deformation. Presumably, in polycrystalline graphite, the slight movement of unit *c*-axis defects releases large numbers of locked-in basal-plane dislocations; thus, the major part of the deformation, even at high temperature, will be shear in the basal plane. The picture is complicated because the deformation is localized and produces void growth.

Neutron irradiation also produces general plastic deformation in polycrystalline graphite (Ref. 13). This distortion has been attributed to a Nabarro mechanism with interstitials, rather than vacancies, acting as the migrating defects. It should also be noted that, as well as producing interstitials, there is some evidence (Ref. 14) that irradiation produces collapsed lines of vacancies. This type of defect is really a dipole consisting of two unit

*c*-axis dislocations as described in Fig. 11. These will, of course, act as suitable sinks for interstitials and sources of vacancies, which will become very much more effective at irradiation temperatures at which vacancies — as well as interstitials — can move. At irradiation tempera-

tures below 1,000°C, *D* depends on the mobility of free interstitials, while *l* depends on the concentration of vacancies. Both these factors increase with the irradiation temperature, which explains the observed lack of temperature dependence on creep rate (Ref. 14).

## Appendix

### Etching and Transmission Electron Microscopy of Pyrolytic Carbon

Polarized light microscopy of metallographically polished sections is commonly used for microstructural studies of carbons and graphites. The contrast developed by this technique depends on the optical anisotropy of graphitic carbons and reveals some features of the orientation texture of the specimen. This is very useful for as-deposited and annealed pyrolytic carbons (pyrolytic graphites), but the very high degree of preferred orientation developed in hot-deformed pyrolytics renders them nearly featureless under polarized light. An etching treatment is, therefore, desirable for such samples, and the ion-bombardment (cathodic) etching technique was attempted. For higher resolution examination than is possible with optical micrography, electron microscopy may be used. Because of its low atomic number, graphite is very well suited for viewing in transmission. The major problem is then preparation of suitable, very thin sections. Some successful techniques are described.

#### A. Cathodic Etching

It is well established that some details of the microstructure of carbons and graphites can be revealed by bombarding a polished surface with inert gas ions (Refs. A-1 to A-3). However, the detailed technique, and the results, seem to vary widely from one practitioner to another. Pyrolytic carbon specimens, in standard plastic metallographic amounts, were connected to the cathode of a high-voltage vacuum discharge system. The system was evacuated and back-filled with argon at a pressure of  $1$  to  $3 \times 10^{-2}$  torr, then a high voltage was applied across the electrodes until a glow discharge started. The etched, pyrolytic carbon surface shown in Fig. A-1 is typical of the patterns revealed by this method. The specimen is a longitudinal section – extending from the grip region into the uniform gage region – of a tensile specimen elongated about 10% in creep under a stress of 10,000 lb/in.<sup>2</sup> at 2600°C. Etching was carried out at 3 kV and 2 mA for 10 min at  $3 \times 10^{-2}$  torr of argon. The photograph was made with polarized light. Etch lines seem to run parallel to the basal planes along the length of the specimen. The lines follow the growth cone contours of the as-deposited structure in the grip region and flatten out in the deformed throat and gage regions. The lines are often discontinuous at the scratch, but closely

follow the change in layer plane orientation at the kink band in the throat region (shown at high magnification in Fig. A-2).

Both the depth-of-field effects at high magnification and the behavior on repolishing showed that the etched lines were grooves. No rational explanation could be found for the highly localized etch pattern. Varying the argon pressure, voltage and time – either independently or simultaneously – had no effect on the etched structures. Time did not permit investigation of etching effects with heavier inert gases such as krypton or xenon.

#### B. Thin Sections

Several techniques for preparing thin sections of pyrolytic carbon for transmission microscopy were explored. Pyrolytic carbon is readily cleaved into thin sheets, but care must be taken not to deform the delicate microscope specimens; such deformation would introduce dislocations and change the original structure, especially in well-graphitized material. The easiest method is to cleave a small piece of graphite many times between strips of tape until a thin portion remains. The remaining section can be separated from the tape by dissolving the glue in amyl acetate. Unfortunately, this method introduces many dislocations, as shown in Fig. A-3. Dislocation production can be reduced by keeping one section of the graphite rigid throughout the many cleavings. One way is to glue the specimen with double-sided tape to a glass slide, then cleave with tape until a thin section remains on the slide.

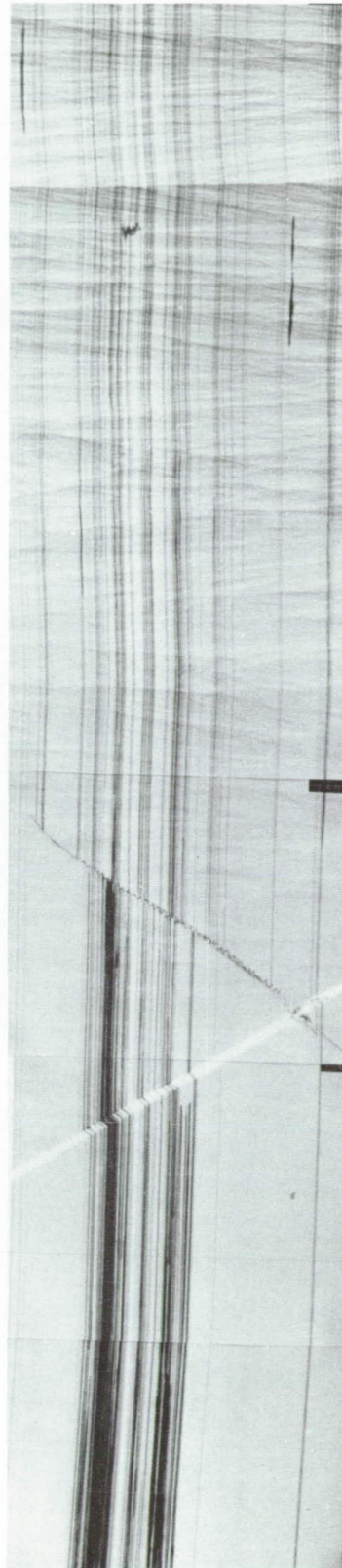
Pyrolytic carbon which has been thinned by mechanical cleaving can be further thinned by playing a small oxygen-hydrogen flame evenly over the surface until small holes begin to appear. This is an adaptation of the technique of Stover (Ref. A-4). When sections of deformed material that have been prepared in this way are observed in the electron microscope, there is an obvious lack of dislocations. However, these specimens will transmit electrons only around the edges of the burnt holes; therefore, the observations are probably biased. Another similar method is to thin a cleaved, thin section by sand



blasting both sides with  $\sim 27\mu$   $\text{Al}_2\text{O}_3$  dust with an air-brasive cutter. Again, the thin sections transmit electrons around hole edges, only. Even though these methods eliminate unwanted dislocations, the action of the beam in the electron microscope seems to generate many more dislocations. For example, the section shown in Fig. A-4 was evenly clear when first viewed in the microscope.

Full exploitation of these techniques was prevented by unavailability of electron microscope facilities at the Jet Propulsion Laboratory. Arrangements were made for use of facilities at the California Institute of Technology, the University of California at Los Angeles, and the University of Southern California for limited observations. Unfortunately, severe restrictions on accessibility and use time and the necessity of using a variety of different microscopes prevented optimum observation techniques.

**Fig. A-1. Cathodically etched, longitudinal section of pyrolytic carbon tensile specimen  
[Polarized light (100 ×)]**



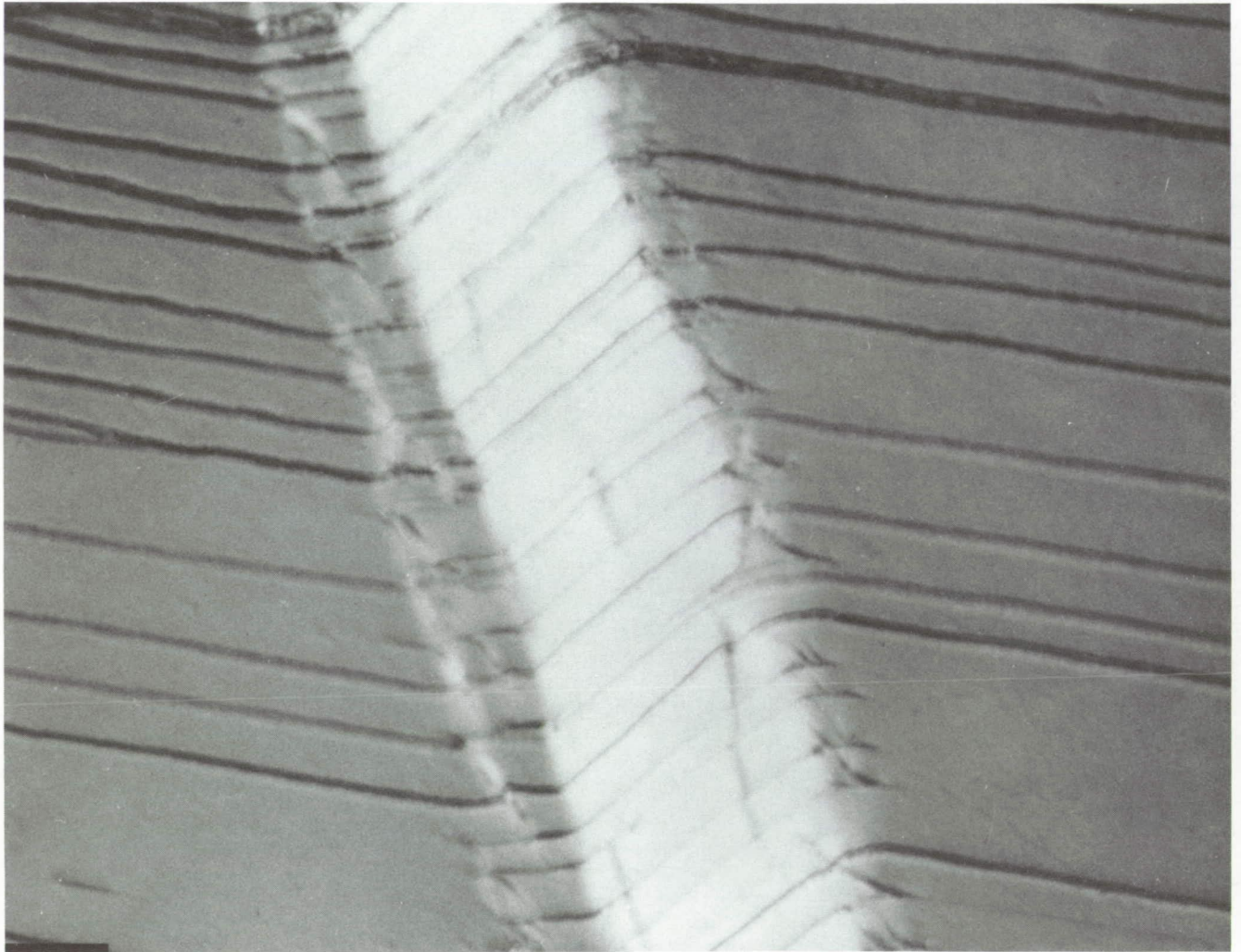
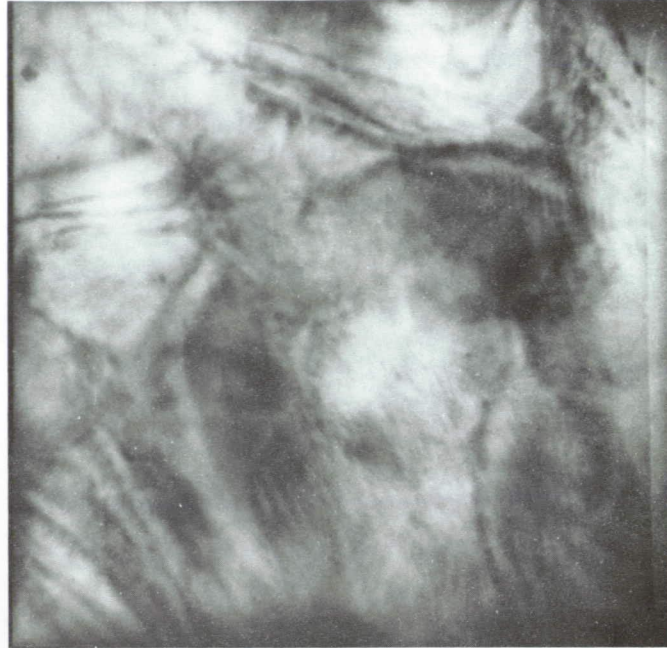


Fig. A-2. Kink band of Fig. 1 (1,000 X)





Fig. A-3. Transmission electron photomicrograph of deformed pyrolytic carbon (20,000 X)



**Fig. A-4. Transmission electron photomicrograph of deformed pyrolytic carbon (21,000 ×)**

### References

1. Kotlensky, W. V., and Martens, H. E., "Mechanical Properties of Pyrolytic Graphite to 2800°C," pp. 625-638 in *Proceedings of the 5th Conference on Carbon, Vol. II*, Pergamon Press, New York, 1963. "Structural Changes Accompanying Deformation in Pyrolytic Graphite," *J. Am. Ceram. Soc.*, Vol. 48, pp. 135-138, 1965.
2. Stover, E. R., "Mechanisms of Deformation and Fracture in Pyrolytic Graphite," *High Temperature Materials II: AIME Conference, Cleveland, Ohio, April 1961, Vol. 18*, pp. 437-453. Edited by G. M. Ault. Interscience Publishers, New York, 1963.
3. Bragg, R. H., Crooks, D. D., Fenn, R. W., Jr., and Hammond, M. L., "Effect of Applied Stress on the Graphitization of Pyrolytic Graphite," *Carbon*, Vol. 1, pp. 171-179, 1964.
4. Fischbach, D. B., and Kotlensky, W. V., "On the Mechanisms of High Temperature Plastic Deformation in Pyrolytic Carbons," *Electrochem. Tech.*, Vol. 5, p. 207, 1967.
5. Sellar, C., and Trillat, J. J., "Reactions des Gas sur le Graphite," *Memoires Scientifiques Rev. Metallurg.*, Vol. 57, p. 187, 1965.

## References (contd)

6. Dienes, G. J., *Mechanism for Self-diffusion in Graphite*, Vol. 23, p. 1194, 1952.
7. Kanter, M. A., "Diffusion of Carbon Atoms in Natural Graphite Crystals," *Phys. Rev.*, Vol. 107, p. 655, 1957.
8. Kotlensky, W. V., "Analysis of High Temperature Creep in Pyrolytic Carbon," *Carbon*, Vol. 4, pp. 209-214, 1966. Also appears as TR 32-889. Jet Propulsion Laboratory, Pasadena, Calif., Feb. 15, 1966.
9. Friedel, J., *Dislocations*, Section 11.3.1. Pergamon Press, New York, 1964.
10. Fischbach, D. B., "Stress Dependence of the Tensile Creep Rate in Carbons and Graphites," Paper MI 42, presented at the 8th Conference on Carbon, Buffalo, June 1967.
11. Jenkins, G. M., and Williamson, G. K., "Deformation and Creep Mechanisms in Graphite," *Proceedings of the Joint International Conference on Creep*, p. 49. Institute of Mechanical Engineering, London, 1963.
12. Green, W. V., and Zukas, E. G., "The Stress Dependence of the Creep Rates of Two Commercial Graphites," *Electrochem. Tech.*, Vol. 5, p. 203, 1967.
13. Jenkins, G. M., and Stephen, D. R., "The Temperature Dependence of the Irradiation Induced Creep of Graphite," *Carbon*, Vol. 4, pp. 67-72, 1956.
14. Horner, P., and Williamson, G. K., "The Effect of the Formation of Vacancy Lines on the Kinetics of Irradiation Damage in Graphite Single Crystals," *Carbon*, Vol. 4, p. 353, 1966.
- A-1. Tarpinian, Aram, "Electrochemical and Ion Bombardment Etching of Pyrolytic Graphite," *J. Am. Ceram. Soc.*, Vol. 47, p. 532, 1964.
- A-2. Reisswig, R. D., Levinson, L. S., and Baker, T. D., "Optical and Electron Microscopy of Carbonaceous Materials," Paper S156, presented at the 8th Conference on Carbon, Buffalo, June 1967.
- A-3. Hales, R. L., and Woodruff, G. M., *Proceedings of the 5th Conference on Carbon, Vol. I*, p. 456. Pergamon Press, New York, 1962.
- A-4. Stover, E. R., "Microscopic Characterization of Layer Stacking in Pyrolytic Graphite," Paper S155, presented at the 8th Conference on Carbon, Buffalo, June 1967.